Improved Efficiency in Hydrogenated Amorphous Silicon Solar Cells Irradiated by Excimer Laser

A. A. Damitha T. Adikaari, S. Ravi P. Silva, Michael J. Kearney and John M. Shannon
Nano-Electronics Centre,
Advanced Technology Institute, University of Surrey,
Guildford, GU2 7XH, United Kingdom.

ABSTRACT

Excimer laser crystallisation is used to fabricate nanocrystalline thin film silicon Schottky barrier solar cells, in a superstrate configuration with indium tin oxide as the front contact and chromium as the back contact. 150 nm thick intrinsic absorber layers are used for the solar cells, and was crystallised using an excimer laser with different laser energy densities. These layers were characterised using Raman spectroscopy and optical absorption before device fabrication. External quantum efficiencies of the devices were calculated from the spectral response data of the devices. A maximum efficiency of 70 % is observed for low energy irradiation, which is significant for very thin absorber layers. Device operation is discussed with proposed band structures for the devices and supplementary measurements.

INTRODUCTION

Excimer laser (EL) crystallisation has been the preferred method for nanocrystalline thin film formation from hydrogenated amorphous silicon (a-Si:H) thin film transistors [1-4]. Pulsed laser energy melts and solidifies thin a-Si:H films within nanosecond time scales, systematically evolving hydrogen and forming nanocrystalline silicon (nc-Si:H). The short wavelength, short pulse duration, ultra violet energy of the excimer lasers is absorbed in the a-Si:H within a few nanometres, with a minimum percentage of heat reaching the substrate. This enables the use of cheap substrates such as glass, which cannot withstand conventional annealing temperatures for large area electronic applications. Although the application has primarily been focused on thin film transistors, its adaptability for photovoltaics has attracted considerable interest over time [5-7]. Significant emphasis has been placed on investigating layered nanocrystalline silicon formation from partially melting a-Si:H using the excimer laser [8,9]. Partial melting occurs when the laser energy density is low, but sufficient to melt a layer of the film, leaving a continuous solid layer underneath. This process results in a stratified structure with large crystallites from the laser irradiated surface, followed by a fine-grained silicon layer. A third unconverted a-Si:H layer is expected at the bottom, depending on how high the laser energy density used, but its properties may be affected due to conducted heat. In this report, we investigate the utilisation of these very thin, stratified nanocrystalline silicon films as absorber layers in Schottky barrier solar cells. The intrinsic nanocrystalline silicon was characterised using Raman spectroscopy and optical absorption measurements before device fabrication. External quantum efficiency (EQE) of the cells was calculated from spectral response of devices and they will be discussed in detail explaining the comparatively high efficiency obtained at low film thickness.

EXPERIMENTAL DETAIL

150 nm thick a-Si:H films were deposited by 13.56 MHz plasma-enhanced chemical vapour deposition at 250ºC. 100 nm thick indium tin oxide (ITO) covered 0.7 mm thick Corning 1737 glass was used as the substrates. A KrF Lambda Physik excimer laser (LPX 210i) operating at 248 nm with 25 ns full width half maximum pulse duration was used to crystallise a-Si:H films. The films were scanned with a 4 mm wide 10 mm in length semi-Gaussian beam profile with the scanning speed at 2.5 mm/s with a pulse repetition rate of 50 Hz, in vacuum (base pressure of 0.0133 Pa) over a total scan area which could be extended to 100x100 mm^2. Scanning of samples was carried out along the Gaussian direction with an overlap of 5% between two scan lines. This arrangement results in a 'multiple pulse irradiation' scheme with a pulse density of 200 at a given spot. The laser energy densities are quoted for a single pulse. A series of laser energy densities were used to crystallise the samples from 40 to 160 $mJcm^{-2}$, in steps of 20 $mJcm^{-2}$. Due to pulse-to-pulse variation of excimer laser energy, the accuracy of energy density measurements is expected to be close to 10% [10].

Chromium back contacts were made to the films, after depositing a heavily phosphorus doped 50 nm thick layer of n-type a-Si:H (n^+ a-Si:H), during the post crystallisation device fabrication process. 500 μm diameter circular chromium contacts were evaporated through a shadow mask and n-type a-Si:H layers surrounding chromium contacts were etched using a plasma etch, in order to reduce leakage currents to a minimum.

Optical transmission measurements of the samples were done with a Camspec M330 UV-visible spectrophotometer, and Raman spectroscopy with a Renishaw 2000 Raman microscope with 782 nm excitation. Current–voltage measurements of the samples were performed using a Kiethley 487 Pico ammeter/Voltage source. EQEs of the devices were calculated from the measurement of spectral response of the devices with a Centronics OSD5.8-7 reference photodiode using a standard lock-in system without a bias light.

RESULTS & DISCUSSION

Material characteristics

Raman spectra for the EL crystallised silicon show a mixed phase silicon spectrum, with increasing crystalline intensities with increased laser energy density [11]. The crystalline volume fractions of the samples were calculated from the integrated intensities of the Raman peaks, with Gaussian fits for amorphous peaks and Lorentzian fits for crystalline peaks. Calculations were performed as proposed by Tsu et al. [12] with the ratio of the backscattering cross sections of amorphous and crystalline phases taken to be 0.8. The technique yields a rough estimate of crystalline to amorphous ratio in the film, where the amorphous contribution results mainly from the unconverted a-Si:H at the bottom layer and some grain boundary contributions. Figure 1 shows the variation of crystalline volume fraction and Tauc gap of EL crystallised silicon with series of laser energy densities. A maximum crystalline volume fraction of 73% resulted at 160 $mJcm^{-2}$. Crystalline volume gradually increases with the increase of EL energy density, which in turn increases the grain boundary density of the film. The amorphous contribution for these films is thought to be from the grain boundaries as well as the unconverted a-Si:H bottom layer.

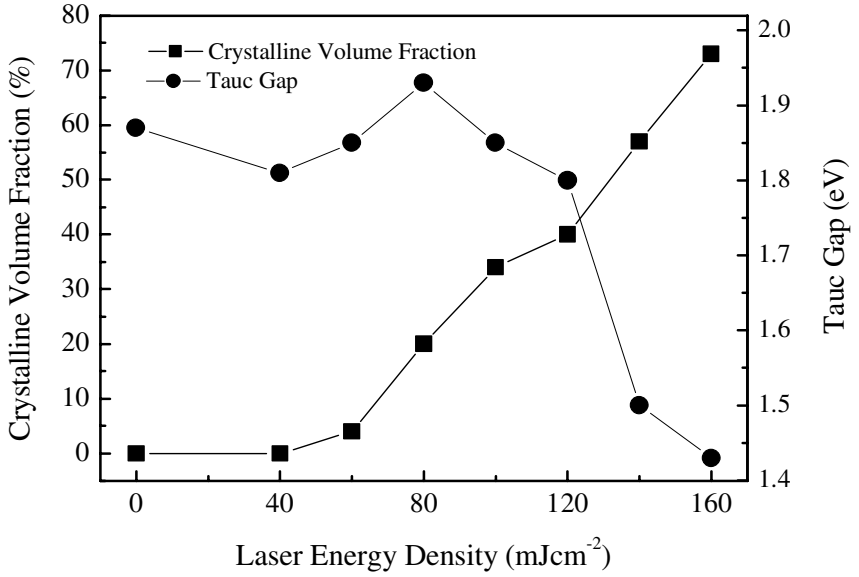

Figure 2. Variation of crystalline volume fraction and Tauc gap of EL crystallised silicon with laser energy density.

The Tauc gap of EL crystallised silicon was estimated by optical absorption measurements and is shown in Figure 1. Due to the stratified nature of the resulting films, the estimated optical gap is a representation of collective absorption of all three different nanocrystalline/amorphous layers. It can be seen that the influence of the amorphous fraction is minimal at laser energy densities above 140 $mJcm^{-2}$, which reduces the optical gap from initially higher values to lower 'composite' bansgaps.

It should be noted that the presence of thin oxide layers both between EL crystallised silicon and n^+a-Si:H layer, and between n^+a-Si:H and chromium back contact is possible. Although crystallisation is done in vacuum, it is expected that there is enough oxygen, for the films to react in the liquid phase. Oxide formation between n^+ a-Si:H and the chromium back contact, which occurs between n^+a-Si:H deposition and metal deposition, is less prominent. The oxide layers are assumed to be transparent to carriers, if present.

Electronic Characteristics

The electronic band structure of the devices was formulated based on the above findings. Figure 2 shows the proposed band structure for the devices under discussion. Depending on the crystallisation energy density, the depth of each type of nanocrystalline layer changes. At higher energy densities, the large grained layer will extend close to the ITO back contact, whereas at lower energy densities, most of the film will be amorphous. The large grained nc-Si:H layer at the laser irradiated surface is assumed to have a lower optical gap than the fine grained nc-Si:H layer sandwiched between this and the unconverted a-Si:H. The fine-grained nc-Si:H layer is expected to have a lower optical gap to a-Si:H. With the work function of ITO approximately 4.7 eV [13] and electron affinity of a-Si:H approximately 4 eV, it is suggested that the a-Si:H makes a Schottky contact to the ITO front contact [14]. The heavily phosphorous doped a-Si:H layer makes a very thin barrier to the Cr back contact, so that carriers tunnel through, resulting in a low

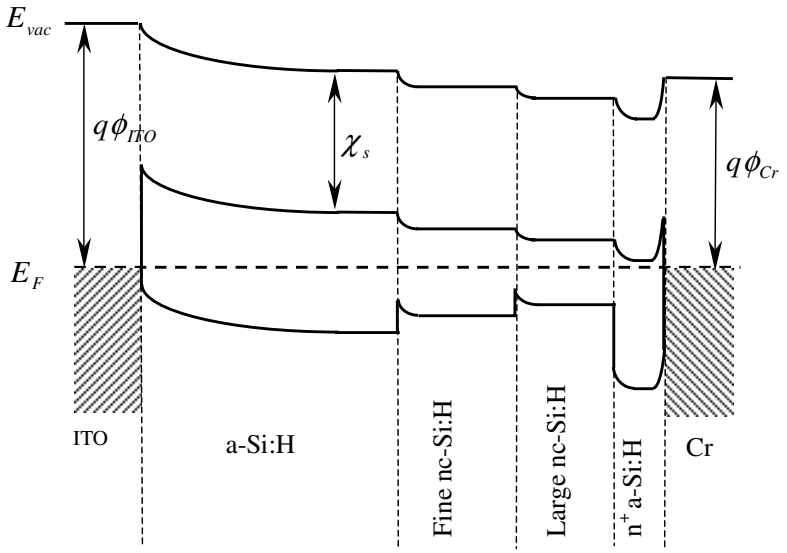

Figure 2. Band structure of EL crystallised silicon Schottky barrier cells indicating work functions of ITO (4.7eV) and Cr (4.5 eV) and electron affinity of a-Si:H (4.0 eV).

resistance back contact. The cascaded band arrangement is expected to aid electron transport upon photo-excitation. From current-voltage measurements of cells, it was observed that the rectifying behaviour of the device is lost after 120 mJ/cm^2 crystallisation energy density. This is thought to be due to considerable structural changes during laser crystallisation. Crystalline volume fractions of these cells are comparatively higher, suggesting increased grain boundary contributions, which increase the conductivity of the films, resulting in near ohmic contacts. Activation energy measurements conducted on these devices confirm this observation, with barrier heights for the ITO/a-Si:H interface calculated to be 0.7 eV for devices made below 120 mJ/cm^2. From the barrier height calculations, it is concluded that the ITO/a-Si:H interface is not significantly affected by the EL treatment up to 100 mJcm^{-2} and the collection mechanisms are similar for all the cells fabricated below this energy.

The EQE of each cell was calculated from the spectral response of the devices within the 300-800 nm wavelengths. Figure 3 shows the EQE plots for devices made with different laser energy densities. The EQE curves show similar spectral response at almost all crystallisation energy densities except for 140 and 160 mJcm^{-2}, where the collection mechanism is insignificantly weak. Three distinct peaks of EQE can be identified for the devices at 330 nm (3.75 eV), 380 nm (3.26 eV), and 475 nm (2.61 eV) wavelengths. It is suggested that the 3. 75 eV peak is due to ITO, where the band gap is around 3.5 eV. [15] The other two peaks are suggested to arise from extended state transitions of the disordered absorber layer. The best EQE corresponds to cells fabricated after crystallising at 40 mJcm^{-2}, with a maximum of 70%, at 475 nm (2.6 eV) of the spectrum. For non-laser treated a-Si:H cells, when the EQE was calculated, it was 30 % at the same wavelength. At 60 and 80 mJcm^{-2} the EQEs are higher than for the amorphous case, however, significantly lower than the 40 mJcm^{-2} devices. With the very thin absorber layers utilised for the cells, this EQE response is significant, compared to previously reported quantum efficiencies of a-Si:H Schottky barrier solar cells. [16]

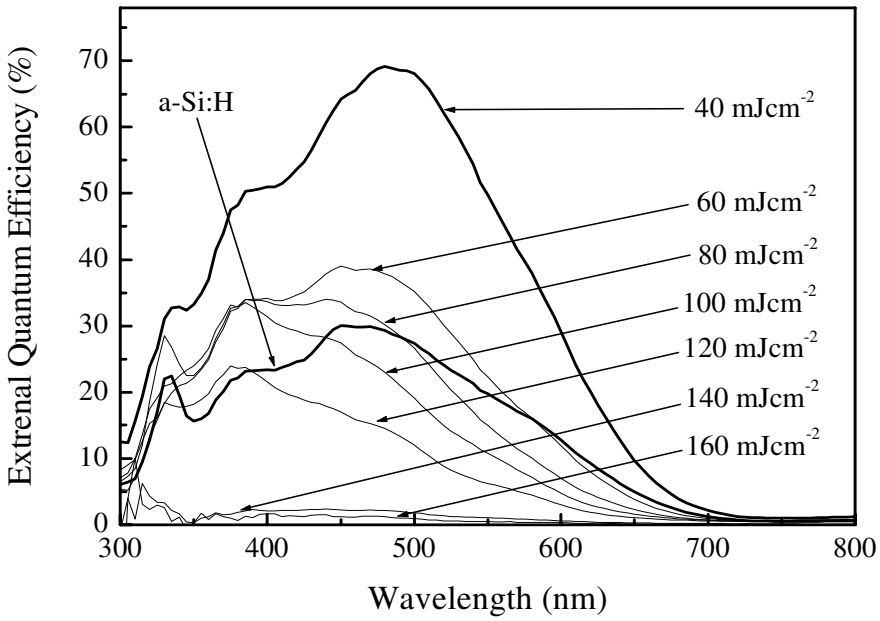

Figure 3. External Quantum efficiency of EL crystallised Schottky barrier cells.

From Figure 1, it is evident that the devices resulting in the highest EQEs show no significant crystalline volume. The whole absorber layer seems to be amorphous, with no apparent changes in optical gap. However, an ultra thin layer of nano crystallites is expected to form at 40 $mJcm^{-2}$ irradiation. This ultra thin layer is expected to have a lower optical gap, higher mobility of carriers with a lower H content compared to rest of the absorber layer. Hence, it is proposed that the efficiency improvements are associated with the interface modification between the absorber layer and the back contact assembly.

CONCLUSION

Very thin Schottky barrier solar cells were fabricated using EL crystallised silicon and ITO on glass superstrates. At 150 nm absorber layer thickness, a maximum EQE of 70% is observed, whereas a-Si:H cells fabricated under the same conditions show 30% EQE. It is concluded that an ultra thin nanocrystalline layer at the back contact assembly from excimer laser treatment improved collection efficiency of photo-generated carriers.

ACKNOWLEDGEMENTS

The authors would like to thank Philips research laboratories, Redhill, Surrey, UK, for the supply of a-Si:H samples and post laser treatment fabrications and G.Y. Chen for Raman measurements. This work is supported by the Portfolio Partnership Award from EPSRC.

REFERENCES

1. S. D. Brotherton, D. J. McCulloch, J. B. Clegg and J. P. Gowers, IEEE Trans. Electron Devices, **40**, 407 (1993).
2. S. D. Brotherton, Semiconductor Science and Technology, **10**, 721 (1995).
3. S. D. Brotherton, D. J. McCulloch, J. P. Gowers, J. R. Ayres and M. J. Trainor, J. Appl. Phys. **82**, 4086 (1997).
4. P. Mei, J. B. Boyce, M. Hack, R. A. Lujan, R. I. Johnson, G. B. Anderson, D. K. Fork and S. E. Ready, Appl. Phys. Lett. **64**, 1132 (1994).
5. H. Azuma, A. Takeuchi, T. Ito, H. Fukushima, T. Motohiro and M. Yamaguchi Solar Energy Materials & Solar Cells, **74**, 289 (2002).
6. K. Yamamoto, A. Nakashima, T. Suzuki, M. Yoshimi, H. Nishio and M. Izumina, Jpn. J. Appl. Phys. **33**, L1751 (1994).
7. Wen-Chang Yeh and M. Matsumura, Jpn. J. Appl. Phys., **38**,L110 (1999).
8. J.S. Im, H. J. Kim and M. O. Thompson, Appl. Phys. Lett. **63**, 1969 (1993).
9. M. O. Thompson, G. J. Galvin, J. W. Mayer, P. S. Peercy, J. M. Poate, D. C. Jacobson, A. G. Cullis and N. G. Chew, Phys. Rev. Lett. **52**, 2360 (1984).
10. A. T. Voustas, Applied surface science, **208-209**, 250 (2003).
11. C. Smit, R. A. C. M. M. van Swaaij, H. Donker and A. M. H. N. Petit, W. M. M. Kessels, and M. C. M. van de Sanden, J. Appl. Phys., **94**, 3582 (2003).
12. R. Tsu, J. Gonzalez-Hernandez, S. S. Chao, S. C. Lee, and K. Tanaka, Appl. Phys. Lett. **40**, 534 (1982).
13. Y. Park, V. Choong, Y. Gao, B. R. Hsieh, and C. W.Tang, Appl. Phys. Lett. **68**, 2699 (1996).
14. Jerzi Kanicki, Appl. Phys. Lett. **53**, 1943 (1988).
15. H. Kim, C. M. Gilmore, A. Piqué, J. S. Horwitz, H. Mattoussi, H. Murata, Z. H. Kafafi, and D. B. Chrisey, J. Appl. Phys., 86, 6451 (1999).
16. D. Gutkowicz-Krusin, C. R. Wronski, and T. Tiedje, Appl. Phys. Lett. 38, 87 (1981).